

Degradation of organic pollutants using metal-doped TiO₂ photocatalysts under visible light: a comparative study

Khalid Umar^{a,*}, Tabassum Parveen^b, Meraj Alam Khan^c, Mohamad Nasir Mohamad Ibrahim^{a,*}, Akil Ahmad^d, Mohd Rafatullah^d

^a*School of Chemical Sciences, Universiti Sains Malaysia, 11800 Pulau Pinang, Malaysia, Tel. +60 4 6533554; Fax: +60 4 6574854; emails: khalidumar@usm.my (K. Umar), mnm@usm.my (M.N.M. Ibrahim)*

^b*Department of Botany, Aligarh Muslim University, Aligarh, India*

^c*Department of Chemistry, Aligarh Muslim University, Aligarh, India*

^d*School of Industrial Technology, Universiti Sains Malaysia, 11800 Pulau Pinang, Malaysia*

Received 30 November 2018; Accepted 18 April 2019

ABSTRACT

Various concentrations of dopants such as Mn, La, and Mo (0.25%–0.1%) were doped into TiO₂ particles. An improved sol-gel method was used to prepare these particles using titanium isopropoxide as a precursor and their photocatalytic activity was tested by studying the degradation of three different types of organic pollutants (acid blue 129, tinidazole, and metalaxyl). The prepared samples were characterized with standard analytical techniques such as X-ray diffraction (XRD), scanning electron microscopy (SEM), and UV–Vis spectroscopy. The XRD analysis suggests the anatase phase with a crystalline nature. The SEM image of undoped TiO₂ exhibits high roughness and irregular shaped particles. The doped TiO₂ particles showed smaller size than undoped TiO₂ with regular shaped and high surface area. The doped TiO₂ particles also show lower band gap energy than undoped. The photocatalytic results indicate that TiO₂ with a dopant concentration of 0.75% for all metal ions shows the highest photocatalytic activity. Moreover, the Mn-doped TiO₂ (0.75%) degraded metalaxyl more efficiently as compared with other studied pollutants.

Keywords: Degradation; Doped TiO₂; Pesticide; Drug; Dye; Visible light

1. Introduction

Although chemical based industries (specially dyes, drugs and pesticides etc.) play a considerable role in human civilization but extensive anthropogenic and industrial activities have introduced large quantities of chemicals in the environment causing potential harm to ecosystems [1]. For example, water soluble compounds such as pesticides, surfactants, dyes, drugs, etc. are mainly responsible to aquatic pollution and thus, becoming a major source of environmental contamination. The presence of these pollutants in water bodies has become a serious challenge

for environmental scientist [2,3] as these pollutants create health problems for human beings and can pollute our ecosystem even if present in trace amount. In the category of drugs, the compounds such as antibiotics, steroids, and hormones have been detected in water systems [2]. The world-wide annual production of dyes is over 70,000 tons, 12% of which is vanished during process of dyeing in the color industry which ultimately pollutes our aquatic environment [3]. Moreover, a large amount of pesticides have been detected in water bodies including ground and surface water throughout the world [4–7]. Due to presence of these contaminants, water is not suitable for domestic use or

* Corresponding authors.

irrigation. Before discharging these contaminated water into the environment, there is a need to remove these pollutants using appropriate methods.

From the last few decades, photocatalytic technique has been emerged as a potential process for degradation of various pollutants (organic and inorganic) from the aqueous medium [7–14]. This technique involves the semiconductor particles under UV light illumination. Several metal oxides (ZrO_2 , TiO_2 , ZnO , SnO_2), metal chalcogenides (ZnS , CdS , $CdSe$) and their combinations have been examined for the degradation of various contaminants. Out of these metal oxide semiconductor particles, TiO_2 is one of the most applied materials in the field of photocatalytic action due to its peculiar characteristics such as biologically and chemically inert, strong resistant toward acidic and basic environment and stable under illumination [15]. The conduction band and valence band energies for TiO_2 have been estimated up to +3.0 and -0.1 V, respectively. The estimated band gap energy is 3.2 eV which indicates that it absorbs near-UV light ($\lambda < 387$ nm) and is not suitable to absorb visible light [16]. To conquer this problem, the doping of metal–non metal ions in TiO_2 has received great attention. Many researchers reported the doping of metals and non-metal into TiO_2 in literature [17–23]. The mechanism of doped TiO_2 under visible region is shown in Fig. 1. Moreover, there are very few literature reports available for the synthesis of Mn, La, and Mo-doped TiO_2 for the photocatalytic degradation of different organic pollutants [24–32]. The doping of metal ions into titania has been proved to be an effective method to enhance its activity in visible light region by delaying the process of recombination [33,34]. The formation of Ti^{3+} ions increases as a result of doping with metal ion which is responsible for the enhancement of photocatalytic activity. Furthermore, Ti^{3+} is also responsible to cause more oxygen defects which facilitate the efficient adsorption of oxygen on the photocatalyst surface [35]. Moreover, the redox energy states of many metal ions exist within the band gap states of catalyst, this introduces new bands within the states of photocatalyst so that it becomes visible light active [20].

Therefore, this work deals with the doping of different metal ions into TiO_2 photocatalyst to make it visible light responsive using a simple modified sol-gel method. The synthesized material was characterized with different analytical techniques and the photocatalytic activities were tested for

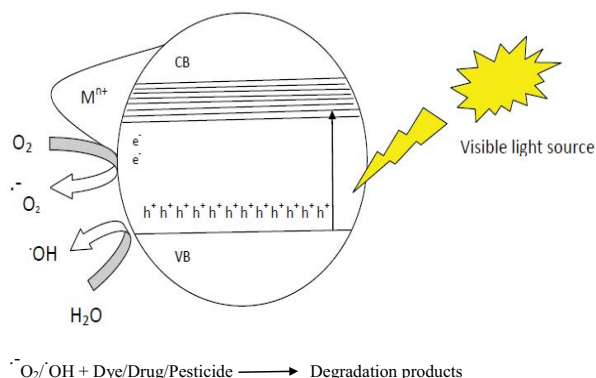


Fig. 1. Mechanism of doped TiO_2 particle (general) for the degradation of organic pollutants.

the degradation of various organic pollutants (tinidazole [drug], metalaxyl [pesticide], and Acid Blue 129 [dye]).

2. Experiment

2.1. Reagents and chemicals

Titanium isopropoxide, Triton-X, acid blue 129, tinidazole and metalaxyl were procured from Sigma-Aldrich, India. Manganese (II) sulphate monohydrate (Himedia Laboratories Pvt. Ltd., India), Ammonium heptamolybdate tetrahydrate (Merck, India), 2-propanol, and lanthanum nitrate hexahydrate were obtained from Central Drug House, India.

2.2. Preparation of undoped and doped TiO_2

Titanium isopropoxide was used as titania precursor to synthesize TiO_2 nanoparticles. In first step of synthesis, titanium precursor/Triton-X was taken in a beaker A and water/2-propanol in other beaker B. In second step, the solution of beaker B was added drop-wise to beaker A at constant stirring. After some times, a turbid solution was appeared which indicates the hydrolysis of titanium precursor, that is, titanium isopropoxide. For next procedure (hydrothermal treatment), obtained materials were transferred into a flask (100 mL) and autoclaved at 350°C for 5 h using Teflon-lined vessel. After that, centrifugation and washing were carried out to remove the impurities. The products were dried in an oven at 50°C for 2 h, and TiO_2 powder was obtained.

For obtaining doped TiO_2 , the whole procedure was same except addition of Mn, Mo and La metal ions by taking the known concentration of their salts, that is, manganese (II) sulphate monohydrate, ammonium heptamolybdate tetrahydrate and lanthanum nitrate hexahydrate.

2.3. Catalysts characterization

To characterize the synthesized catalysts, different analytical techniques such as UV–Vis spectroscopy, X-ray diffraction (XRD) and scanning electron microscopy (SEM) were used. Structural properties of doped and undoped TiO_2 were examined XRD (2θ range of 20° to 80° with Cu $K\alpha$ radiations ($\lambda = 1.5418$ Å)). It was operated at a voltage of 30 kV and current of 15 mA. UV–Vis spectrophotometer (model 1601, Shimadzu, Japan) was used to record the UV–Vis spectra over 300–800 nm range. The surface morphology of synthesized catalysts was studied using SEM (LEO, 435 VF). Transmission electron microscopy (TEM) analysis was performed on a Jeol H-7500 microscope (Japan).

2.4. Photocatalytic experiments

In this study, a photochemical reactor made of Pyrex glass was used. The solution of the desired concentrations of different pollutants such as acid blue 129, tinidazole and metalaxyl were prepared in demineralized water. The aqueous solution of pollutant was fixed into the reactor and added the photocatalyst materials in required amount for the irradiation experiments. The respective solution was agitated and aerated with atmospheric oxygen using a pump throughout the experiment. Prior to illumination, the model pollutant

was continuously stirred in the dark for at least 15 min to the system. Visible light halogen lamp (500 W, 9,500 Lu) was used in this study for irradiation process. During the treatment process, samples were collected at regular time interval and the solution was centrifuged before the compound analysis.

UV-Vis spectrophotometry was used to analyze the absorbance of different pollutants (acid blue 129, tinidazole and metalaxyl) at their respective λ_{\max} . The pollutant concentrations were obtained by plotting the standard calibration curve. This curve was plotted by taking the absorbance of known concentration of respective pollutants.

For every experiment, a plot has been drawn between natural logarithm of concentration/time and evaluated the rate constant. The equation use for calculating the rate of degradation is given below:

$$\frac{-d[C]}{dt} = kC^n \quad (1)$$

where C represents the concentration of pollutants, k represents the rate constant, and n represents the order of reaction. The rate of degradation of pollutants was represented in terms of $\text{mol L}^{-1} \text{min}^{-1}$.

3. Results and discussion

3.1. Catalysts characterization

The XRD patterns of the synthesized doped and undoped TiO_2 with various concentrations of Mn, Mo, and La, which was calcinated at 350°C for 5 h, were analyzed and are depicted in Figs. 2–4. After the sample analysis, the peaks were appeared in the respective crystal planes which are (101), (103), (004), (112), (200), (105), (211), (118) (116), and (220). These patterns exhibited the crystalline nature and anatase phase of doped and undoped TiO_2 [32]. Among all metal-doped TiO_2 , Mn-doped TiO_2 shows more crystalline nature as compared with others. From the XRD patterns, it was observed that there is no significant change in doped and undoped TiO_2 lattice which may be due to the low concentration of dopant as compared with TiO_2 concentration. Moreover, the ionic radii of titanium Ti^{4+} (0.060 \AA) and

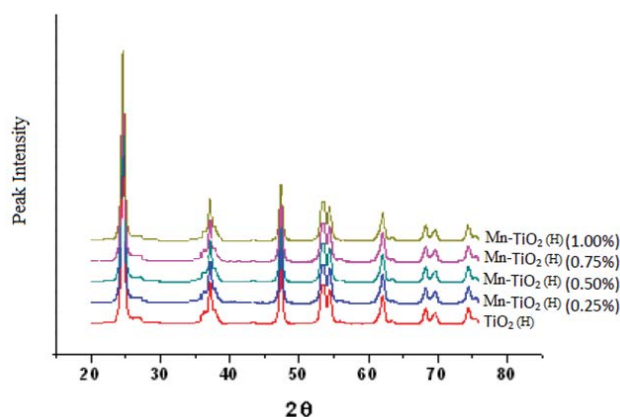


Fig. 2. XRD patterns of undoped TiO_2 and Mn-doped TiO_2 (0.25%, 0.50%, 0.75%, and 1.0%).

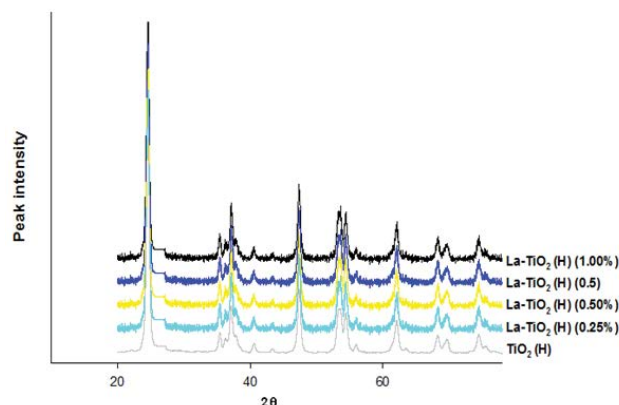


Fig. 3. XRD patterns of undoped TiO_2 and La-doped TiO_2 (0.25%, 0.50%, 0.75%, and 1.0%).

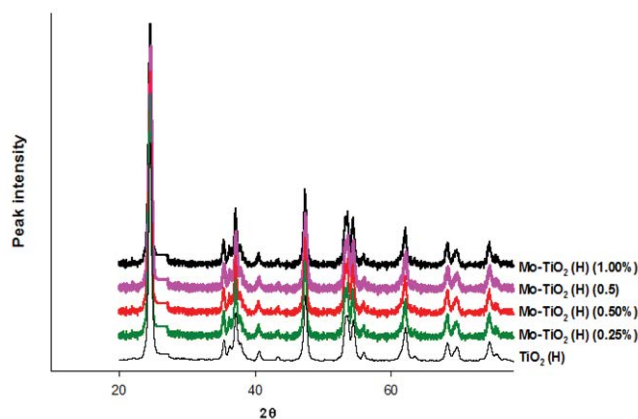


Fig. 4. XRD patterns of undoped TiO_2 and Mo-doped TiO_2 (0.25%, 0.50%, 0.75%, and 1.0%).

the doped metal ion Mo^{6+} (0.620 \AA) are comparable, therefore Ti^{4+} can be replaced by Mo^{6+} in the crystal lattice [25]. Furthermore, Ti^{4+} (0.060 \AA) have lower lattice as compared with La^{3+} (0.101 \AA) and Mn^{2+} (0.080 \AA). Due to the large size of these dopants, it cannot act as interstitial impurities and may appear on the TiO_2 surface [28,29].

UV-Vis light excitation creates photogenerated holes and electrons in the band structure of used materials. The UV-Vis absorption spectra were evaluated of undoped and doped TiO_2 by varying the concentration of dopants. The spectra of undoped and Mn-doped TiO_2 are represented in Fig. 5. The following equation was applied for the band gap evaluation of absorption spectra of undoped and doped TiO_2 .

$$\text{Band energy (eV)} = \frac{1,240}{\text{wavelength (nm)}} \quad (2)$$

The band gap energies are found to be as follows: undoped TiO_2 (3.18 eV), 0.25% Mn-doped TiO_2 (3.05 eV), 0.50% Mn-doped TiO_2 (2.93 eV), 0.75% Mn-doped TiO_2 (2.72 eV), 0.10% Mn-doped TiO_2 (2.80 eV). A red shift (UV-Vis absorption spectra) has been observed in band gap transition

of Mn-doped TiO_2 . This may be due to the introduction of new energy level in TiO_2 band gap which is responsible for the decrease in band gap energy and ultimately photocatalyst can work in visible region [36].

The surface morphology of doped and undoped TiO_2 was studied using the SEM technique. Figs. 6a–d depict the

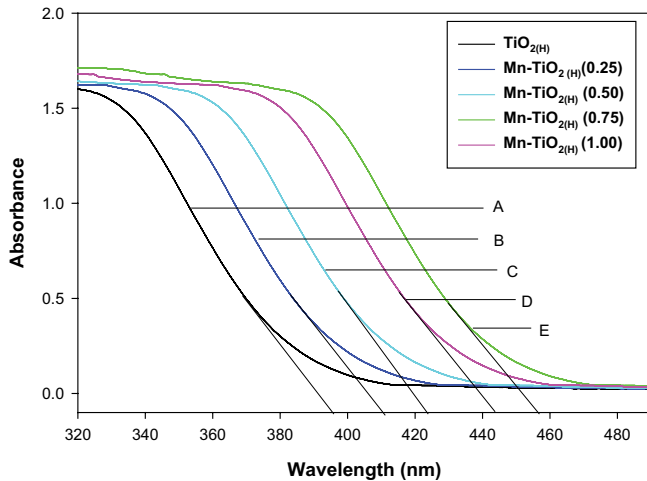


Fig. 5. Absorption spectra of undoped and Mn-doped TiO_2 , (a) Undoped TiO_2 , (b) 0.25% Mn-doped TiO_2 , (c) 0.50% Mn-doped TiO_2 , (d) 1.00% Mn-doped TiO_2 and (e) 0.75% Mn-doped TiO_2 .

surface structure of undoped TiO_2 and other doped TiO_2 , that is, Mn-doped (0.75%), Mo-doped (0.75%) and La-doped (0.75%). The high roughness with relatively large sized particles was observed in case of undoped TiO_2 , while porous and crystalline complex nature with relatively small size particles was observed in case of doped TiO_2 . It was concluded that high surface area observed in case of doped TiO_2 is also responsible for better photocatalytic activities. Furthermore TEM technique was also carried out to analyze the synthesized material. Figs. 7a–d show the TEM images undoped TiO_2 and other doped TiO_2 , that is, Mn-doped (0.75%), Mo-doped (0.75%), and La-doped (0.75%). It can be seen from the figures that the particles of undoped TiO_2 have relatively larger size and irregular in shape and non-uniform distribution of particles. Among all doped TiO_2 , Mn-doped TiO_2 gained smallest, regular spherical shape, and fine distribution of particles, which may be responsible for better photocatalytic activity.

3.2. Photocatalytic application

3.2.1. Photocatalytic action of Mn-doped- TiO_2 for the degradation of various organic pollutants

Acid blue 129 (0.40 mM, 250 mL), tinidazole (1.00 mM, 250 mL) and metalaxyl (1.00 mM, 250 mL) were individually irradiated (visible-light halogen lamp) in an aqueous solution individually in the presence of (1 g L^{-1}) Mn-doped, La-doped,

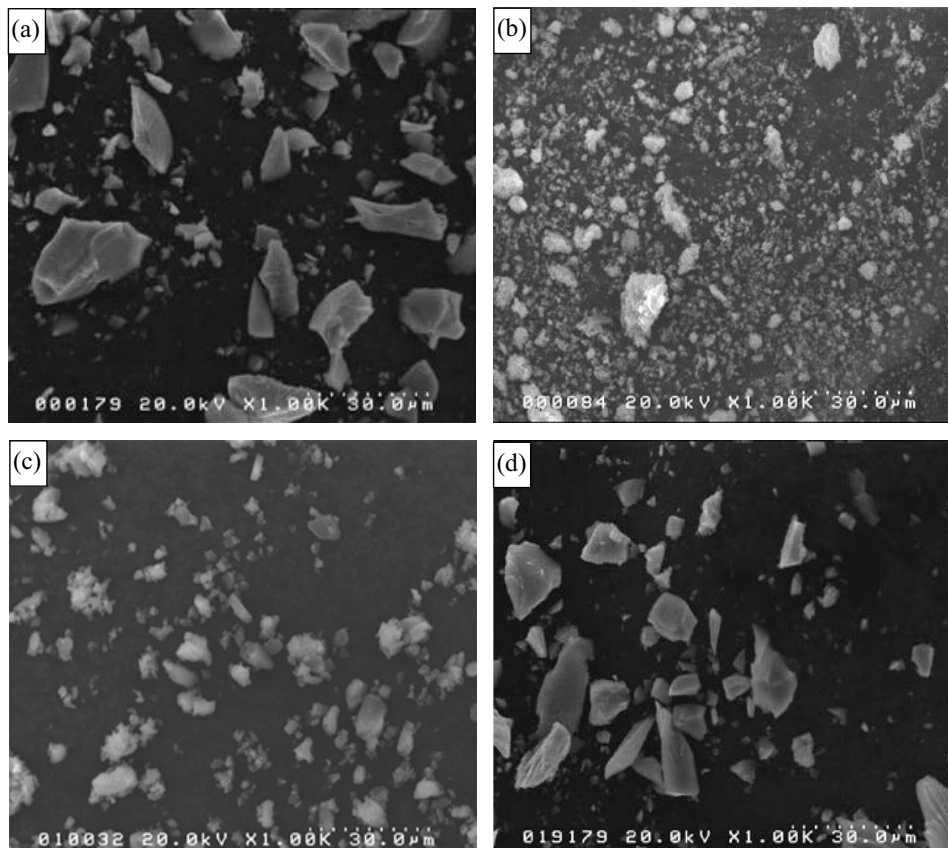


Fig. 6. SEM images of (a) undoped TiO_2 , (b) Mn-doped (0.75%) TiO_2 , (c) La-doped (0.75%) TiO_2 , (d) Mo-doped (0.75%) TiO_2 , calcination temperature: 350°C , calcination time: 5 h.

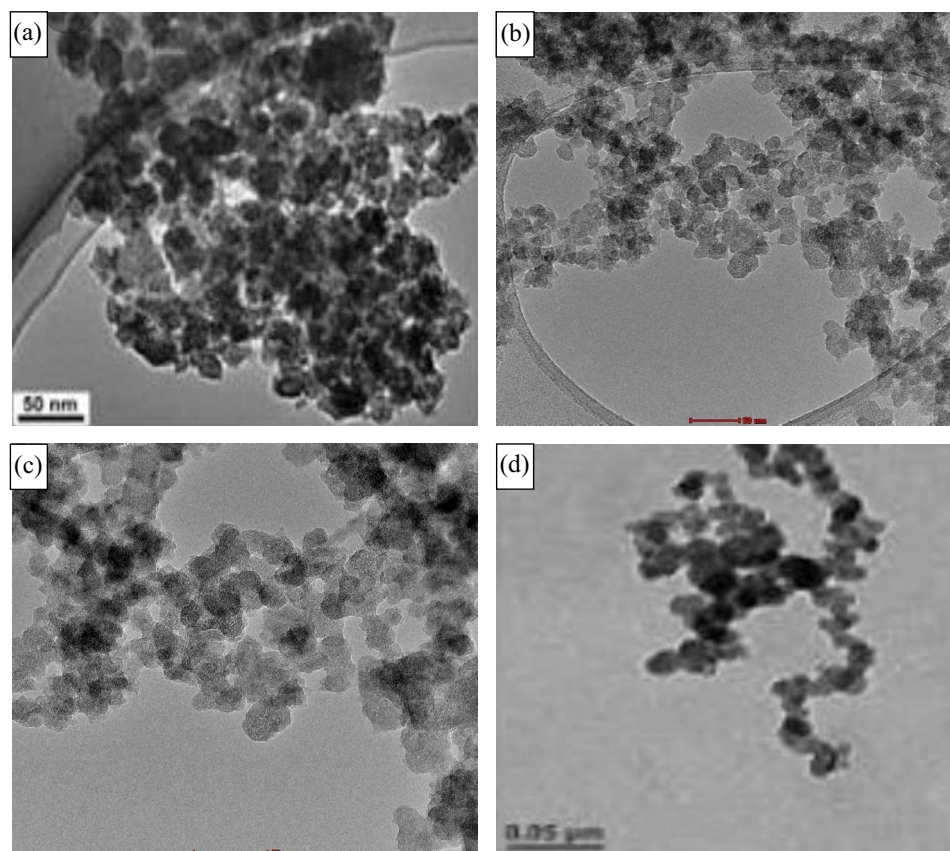


Fig. 7. TEM images of (a) undoped TiO_2 , (b) Mn-doped (0.75%) TiO_2 , (c) La-doped (0.75%) TiO_2 , and (d) Mo-doped (0.75%) TiO_2 , calcination temperature: 350°C , calcination time: 5 h.

and Mo-doped TiO_2 at constant stirring. As a representative example, Fig. 8 depicts the change in pollutants concentration as a function of irradiation time in the presence and absence of 0.75% Mo-doped- TiO_2 (acid blue 129), 0.75% La-doped- TiO_2 (tinidazole), and 0.75% Mn-doped- TiO_2 (metalaxyl). Degradation of acid blue 129, tinidazole, and metalaxyl was found to be 51%, 64%, and 84%, respectively, after irradiation time of 360 min in the presence of Mo-, La-, and Mn-doped TiO_2 . No degradation was observed in the absence of photocatalysts.

To check the photocatalytic activity of different catalysts based on Mn-, La-, and Mo-doped TiO_2 using different concentration (0.25%–1%) have been tested for all three pollutants such as acid blue 129, tinidazole, and metalaxyl under the visible light. The rates of degradation of all pollutants in the presence of doped and undoped TiO_2 are depicted in Figs. 9–11. As shown in figures, it was concluded that the rate of degradation increases with increase in the concentration of dopants (0.25%–0.75%) and decreases with further increase in the dopant concentration. From these results, optimum dose of metals dopant for pollutant degradation was found to be 0.75% and after this the rate of degradation decreased. With increase in concentration of dopant photocatalytic activity increases which may be due to the high surface barrier but with further increase in dopant concentration, photocatalytic activity decreases which may be due to narrower space charge.

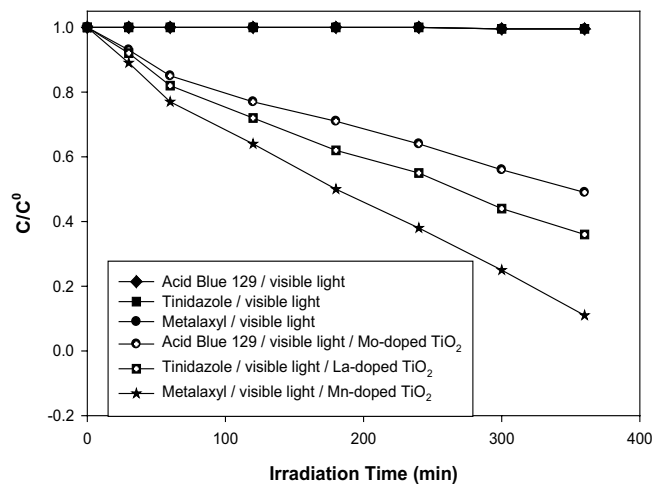


Fig. 8. Change in concentration as a function of time on irradiation of an aqueous solution of acid blue 129, tinidazole, metalaxyl in the absence and presence of Mo-doped TiO_2 , La-doped TiO_2 , Mn-doped TiO_2 , respectively.

Experimental conditions: Reaction vessel: immersion well photochemical reactor made of Pyrex glass, acid blue 129 (0.40 mM), tinidazole (1.00 mM), metalaxyl (1.00 mM) volume (250 mL), Dopant: Mo, Mn, La dopant concentration (0.75%), light source: halogen linear lamp (500 W, 9,500 Lumens) continuous stirring and air purging, irradiation time: 360 min.

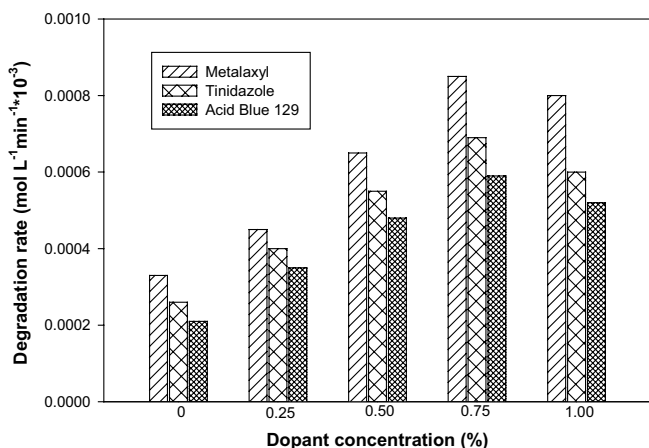


Fig. 9. Photocatalytic activity of Mn-doped TiO₂ for the degradation of metalaxyl, tinidazole, acid blue 129.

Experimental conditions: Reaction vessel: immersion well photochemical reactor made of Pyrex glass, metalaxyl (1.00 mM), tinidazole (1.00 mM), acid blue 129 (0.40 mM), volume (250 mL), Dopant: Mn, Dopant concentration (0, 0.25, 0.50, 0.75, and 1.0%), light source: halogen linear lamp (500 W, 9,500 Lumens) continuous stirring and air purging, irradiation time: 360 min.

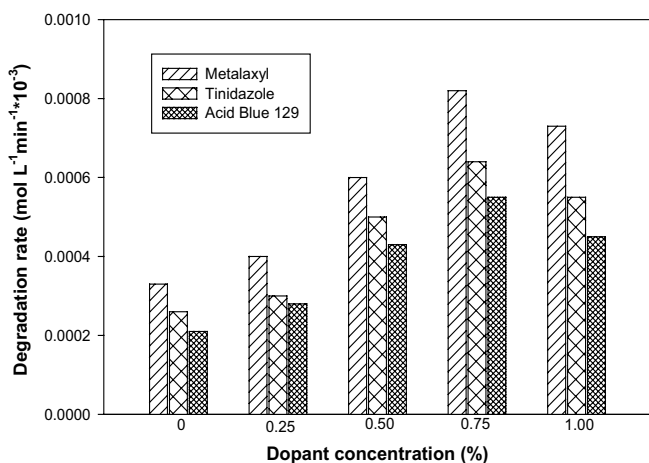


Fig. 10. Photocatalytic activity of La-doped TiO₂ for the degradation of metalaxyl, tinidazole, acid blue 129.

Experimental conditions: Reaction vessel: immersion well photochemical reactor made of Pyrex glass, metalaxyl (1.00 mM), tinidazole (1.00 mM), acid blue 129 (0.40 mM), volume (250 mL), Dopant: La, Dopant concentration (0, 0.25, 0.50, 0.75, and 1.0%), light source: halogen linear lamp (500 W, 9,500 Lumens) continuous stirring and air purging, irradiation time: 360 min.

Due to this, electron–hole pairs are separated well in this region. By this recombination slows down and availability of electron hole pairs in the region occur readily [29]. Nevertheless, dopant concentration increases after achieving the optimal condition due to space charge which is greatly influenced by the penetration of light through TiO₂ and resulting in the increase in surface charge. Hence, generation of electron–hole pairs becomes easier which is responsible for the pollutants degradation and increases the photocatalytic activity of prepared materials [29].

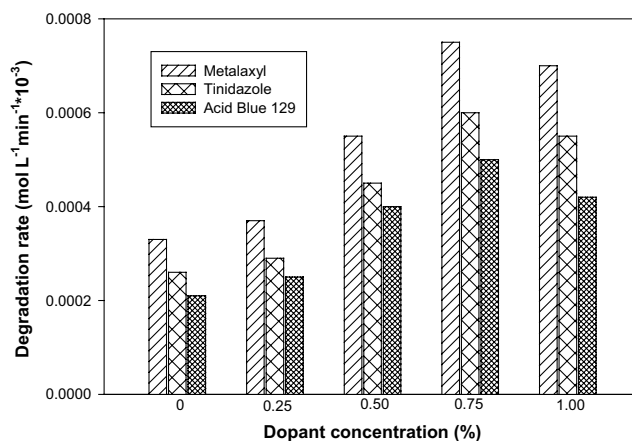


Fig. 11. Photocatalytic activity of Mo-doped TiO₂ for the degradation of metalaxyl, tinidazole, acid blue 129.

Experimental conditions: Reaction vessel: immersion well photochemical reactor made of Pyrex glass, metalaxyl (1.00 mM), tinidazole (1.00 mM), acid blue 129 (0.40 mM), volume (250 mL), Dopant: Mo, Dopant concentration (0, 0.25, 0.50, 0.75, and 1.0%), light source: halogen linear lamp (500 W, 9,500 Lumens) continuous stirring and air purging, irradiation time: 360 min.

All three types of pollutants degradation were studied by taking different metal-based dopants on TiO₂ under similar conditions. Fig. 12 depicts the pattern of degradation of metalaxyl pollutants in the presence of doped TiO₂ (Mn, La, and Mo, 0.75%) as a representative example. From the results, it was found that Mn-doped TiO₂ gives better degradation efficiency for all pollutants as compared with other metals doped TiO₂. Our outcomes in this study are in good agreement with the previous report in literature [37,33]. For example, the photoreactivity of metal ion doped TiO₂ depends on various complex factors such as the distribution

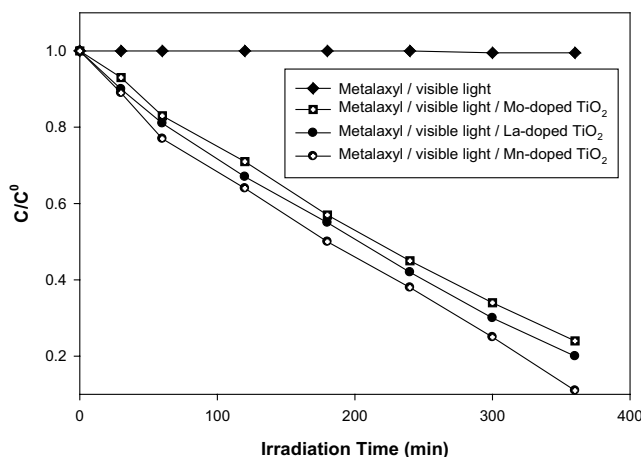


Fig. 12. Change in concentration as a function of time on irradiation of an aqueous solution of metalaxyl in the absence and presence of Mn-doped TiO₂.

Experimental conditions: Reaction vessel: immersion well photochemical reactor made of Pyrex glass, metalaxyl (1.00 mM) volume (250 mL), Dopant: Mn, Dopant concentration (0.75%), light source: halogen linear lamp (500 W, 9,500 Lumens) continuous stirring and air purging, irradiation time: 360 min.

of dopants, dopant concentration, the dopant energy levels within the TiO_2 lattice, the electron donor concentration, their d electronic configuration and also the light intensity. For example, Devi et al. [37] reported that Zn^{2+} doped TiO_2 showed higher activity as compared with V^{5+} doped TiO_2 for the degradation of the same organic pollutant, although both samples showed identical band gap absorption. But the smaller crystallite size of Zn^{2+} doped TiO_2 and the stable filled electronic configuration of the Zn^{2+} ion served as a shallow trap for the charge carriers contributing to the overall activity similar to our studies Mn^{2+} ion exhibit the same. Moreover, the enhanced activity of Mn^{2+} doped TiO_2 as compared with other compared with other transition metal doped TiO_2 (V^{5+} , Fe^{3+} , Ni^{2+} , Zn^{2+} , Os^{3+} , and Ru^{3+}) for the degradation of indigo carmine and 4-CP was reported by Devi et al. [33]. The better activity of Mn^{2+} was attributed to factors as follows: high redox potential of $\text{Mn}^{2+}/\text{Mn}^{3+}$ pairs, unique half-filled electronic structure of Mn^{2+} , which served as a shallow trap for the charge carriers and slows down the recombination process, smaller crystallite size and favorable surface structure of the photocatalyst. Devi et al. [25] studied the photocatalytic activity of Mn- and Mo-doped TiO_2 and reported that Mn-doped TiO_2 shows better photocatalytic activity than Mo-doped TiO_2 . Furthermore, due to unique half-filled electronic configuration of manganese ions (d^5), when ions hold the holes or electrons, half-filled of electronic configuration of metal is upset. Due to this, it might gain the original position and transfer the holes and electrons which create the radicals of hydroxide and superoxide [25].

The photocatalytic activity of synthesized TiO_2 doped with Mn, La, and Mo metal ions was also tested for the degradation of three types of pollutants that were under investigation using visible light. As a representative example, the change in concentration as a function of the irradiation time of an aqueous solution of all the individual compounds in

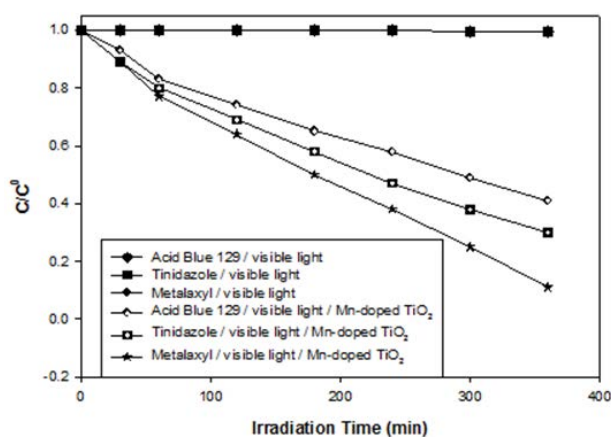


Fig. 13. Change in concentration as a function of time on irradiation of an aqueous solution of acid blue 129, tinidazole, metalaxyl in the absence and presence of Mn-doped TiO_2 .

Experimental conditions: Reaction vessel: immersion well photochemical reactor made of Pyrex glass, acid blue 129 (0.40 mM), tinidazole (1.00 mM), metalaxyl (1.00 mM), volume (250 mL), Dopant: Mn, dopant concentration (0.75%), light source: halogen linear lamp (500 W, 9,500 Lumens) continuous stirring and air purging, irradiation time: 360 min.

the presence of Mn-doped (0.75%) TiO_2 is shown in Fig. 13. The result shows that the degradation patterns of the three pollutants follow the order: acid blue 129 < tinidazole < metalaxyl. The slowest degradation of acid blue 129 is attributed to its classification in the category of anthraquinone dyes. Anthraquinone dyes contain fused aromatic rings that remain intact for longer time during the degradation process. Our results are consistent with a previous study [38]. The better degradation rate of metalaxyl may also be attributed to the fact that the structural orientation of this compound is favored for the attack of the reactive species under these conditions.

4. Conclusion

Different concentrations of dopant such as Mn, La, and Mo (0.25%–1.0%) were doped on TiO_2 particles. The photocatalytic activity was studied for degradation of three different types of pollutants. XRD analysis was applied to find the anatase phase with crystalline nature of synthesized materials. In case of undoped TiO_2 , high roughness, and irregular shaped particles were observed in SEM image while smaller size, regular spherical shaped particles was observed in case of doped TiO_2 . The photocatalytic outcomes indicate that TiO_2 with 0.75% dopant concentration for Mn, La, and Mo metal has maximum photocatalytic performance using visible light. Amongst all the pollutants studied, the metalaxyl has a better degradation rate than the other pollutants. Mn ions have the best photocatalytic activity among all dopants because of its unique half-filled electronic configuration.

Acknowledgments

The authors gratefully acknowledged the post doctoral financial support (USM/PPSK/FPD(BW) 1/06 (2018) and a research university individual grant scheme (1001/PKIMIA/8011070) by Universiti Sains Malaysia.

References

- [1] C.M. Teh, A.R. Mohamed, Roles of titanium dioxide and ion-doped titanium dioxide on photocatalytic degradation of organic pollutants (phenolic compounds and dyes) in aqueous solutions: a review, *J. Alloys Compd.*, 509 (2011) 1648–1660.
- [2] D.W. Kolpin, E.T. Furlong, M.T. Meyer, E.M. Thurman, S.D. Zaugg, L.B. Barber, H.T. Buxton, Pharmaceuticals, hormones, and other organic wastewater contaminants in U.S. streams, 1999–2000: a national reconnaissance, *Environ. Sci. Technol.*, 36 (2002) 1202–1211.
- [3] K. Umar, A.A. Dar, M.M. Haque, N.A. Mir, M. Muneer, Photocatalysed decolourization of two textile dye derivatives, Martius Yellow and Acid Blue 129, in UV-irradiated aqueous suspensions of Titania, *Desal. Wat. Treat.*, 46 (2012) 205–214.
- [4] K.L. Knee, R. Gossett, A.B. Boehm, A. Paytan, Caffeine and agricultural pesticide concentrations in surface water and groundwater on the north shore of Kauai (Hawaii, USA), *Mar. Pollut. Bull.*, 60 (2010) 1376–1382.
- [5] STORET Water Quality File, Office of Water, U.S. Environmental Protection Agency Data File Search Conducted in March, May, 1988.
- [6] M.G. Rovedatti, P.M. Castane, M.L. Topalián, A. Salibián, Monitoring of organochlorine and organophosphorus pesticides in the water of the Reconquista river (Buenos Aires, Argentina), *Water Res.*, 35 (2001) 3457–3461.

- [7] D.M. Blake, Bibliography of Work on the Photocatalytic Removal of Hazardous Compounds from Water and Air, National Renewable Energy Laboratory, Colorado, USA, 2001.
- [8] B. Neppolian, H.C. Choi, S. Sakthivel, B. Arabindoo, V. Murugesan, Solar/UV-induced photocatalytic degradation of three commercial textile dyes, *J. Hazard. Mater.*, 89 (2002) 303–317.
- [9] J. Xu, Y. Ao, M. Chen, D. Fu, Low-temperature preparation of Boron-doped titania by hydrothermal method and its photocatalytic activity, *J. Alloys Compd.*, 484 (2009) 73–79.
- [10] S. Liu, X. Liu, Y. Chen, R. Jiang, A novel preparation of highly active iron-doped titania photocatalysts with a p–n junction semiconductor structure, *J. Alloys Compd.*, 506 (2010) 877–882.
- [11] T. Sano, E. Puzenat, C. Guillard, C. Geantet, S. Matsuzawa, Degradation of C₂H₂ with modified-TiO₂ photocatalysts under visible light irradiation, *J. Mol. Catal. A: Chem.*, 284 (2008) 127–133.
- [12] K. Umar, M.M. Haque, N.A. Mir, M. Muneer, Titanium dioxide-mediated photocatalysed mineralization of two selected organic pollutants in aqueous suspensions, *J. Adv. Oxid. Technol.*, 16 (2013) 252–260.
- [13] U.G. Akpan, B.H. Hameed, Parameters affecting the photocatalytic degradation of dyes using TiO₂-based photocatalysts: a review, *J. Hazard. Mater.*, 170 (2009) 520–529.
- [14] I.A. Alaton, I.A. Balcioglu, D.W. Bahnemann, Advanced oxidation of a reactive dye bath effluent: comparison of O₃, H₂O₂/UV-C and TiO₂/UV-A processes, *Water Res.*, 36 (2002) 1143–1154.
- [15] M.A. Fox, M.T. Dulay, Heterogeneous photocatalysis, *Chem. Rev.*, 93 (1993) 341–357.
- [16] B. Shahmoradi, M.A. Pordel, M. Pirsaeheb, A. Maleki, S. Kohzadi, Y. Gong, R.R. Pawar, S.-M. Lee, H.P. Shivaraju, G. McKay, Synthesis and characterization of barium-doped TiO₂ nanocrystals for photocatalytic degradation of Acid Red 18 under solar irradiation, *Desal. Wat. Treat.*, 88 (2017) 200–206.
- [17] K. Umar, M.M. Haque, M. Muneer, T. Harada, M. Matsumura, Mo, Mn and La doped TiO₂: Synthesis, characterization and photocatalytic activity for the decolorization of three different chromophoric dyes, *J. Alloys Compd.*, 578 (2013) 431–438.
- [18] T.S. Jamil, T.A. Gad-Allah, M.Y. Ghaly, Parametric study on phenol photocatalytic degradation under pure visible and solar irradiations by Fe-doped TiO₂, *Desal. Wat. Treat.*, 50 (2012) 264–271.
- [19] W. Raza, M.M. Haque, M. Muneer, T. Harada, M. Matsumura, Synthesis, characterization and photocatalytic performance of visible light induced bismuth oxide nanoparticle, *J. Alloys Compd.*, 648 (2015) 641–650.
- [20] V.D. Binas, K. Sambani, T. Maggos, A. Katsanaki, G. Kiriakidis, Synthesis and photocatalytic activity of Mn-doped TiO₂ nanostructured powders under UV and visible light, *Appl. Catal., B*, 113–114 (2012) 79–86.
- [21] W. Raza, M.M. Haque, M. Muneer, Synthesis of visible light driven ZnO: characterization and photocatalytic performance, *Appl. Surf. Sci.*, 322 (2014) 215–224.
- [22] S. Ata, M.Z. Ullah, M.I. Din, R. Mehmood, W. Farooq, S.A. Trimzi, I. Bibi, Novel synthesis and enhanced catalytic performance of stable nano-scale Fe⁰, Ag⁰ and ZnO nanoparticles: photo-degradation under mercury lamp, *Desal. Wat. Treat.*, 131 (2018) 212–219.
- [23] B. Shahmoradi, A. Maleki, K. Byrappa, Removal of Disperse Orange 25 using *in situ* surface-modified iron-doped TiO₂ nanoparticles, *Desal. Wat. Treat.*, 53 (2015) 3615–3622.
- [24] L.G. Devi, B.N. Murthy, Characterization of Mo doped TiO₂ and its enhanced photo catalytic activity under visible light, *Catal. Lett.*, 125 (2008) 320–330.
- [25] L.G. Devi, S.G. Kumar, B.N. Murthy, N. Kottam, Influence of Mn²⁺ and Mo⁶⁺ dopants on the phase transformations of TiO₂ lattice and its photo catalytic activity under solar illumination, *Catal. Commun.*, 10 (2009) 794–798.
- [26] V.C. Papadimitriou, V.G. Stefanopoulos, M.N. Romanias, P. Papagiannakopoulos, K. Sambani, V. Tudose, G. Kiriakidis, Determination of photo-catalytic activity of un-doped and Mn-doped TiO₂ anatase powders on acetaldehyde under UV and visible light, *Thin Solid Films*, 520 (2011) 1195–1201.
- [27] M. Jin, Y. Nagaoka, K. Nishi, K. Ogawa, S. Nagahata, T. Horikawa, M. Katoh, T. Tomida, J. Hayashi, Adsorption properties and photocatalytic activity of TiO₂ and La-doped TiO₂, *Adsorption*, 14 (2008) 257–263.
- [28] T. Peng, D. Zhao, H. Song, C. Yan, Preparation of lanthanum-doped titania nanoparticles with anatase mesoporous walls and high photocatalytic activity, *J. Mol. Catal. A: Chem.*, 238 (2005) 119–126.
- [29] V. Štengl, S. Bakardjieva, N. Murafa, Preparation and photocatalytic activity of rare earth doped TiO₂ nanoparticles, *Mater. Chem. Phys.*, 114 (2009) 217–226.
- [30] J. Liqiang, S. Xiaojun, X. Baifu, W. Baiqi, C. Weimin, F. Hong-gang, The preparation and characterization of La doped TiO₂ nanoparticles and their photocatalytic activity, *J. Solid State Chem.*, 177 (2004) 3375–3382.
- [31] H. Chen, M. Shen, R. Chen, K. Dai, T. Peng, Photocatalytic degradation of commercial methyl parathion in aqueous suspension containing La-doped TiO₂ nanoparticles, *Environ. Technol.*, 32 (2011) 1515–1520.
- [32] W. Raza, M.M. Haque, M. Muneer, M. Fleisch, A. Hakki, D. Bahnemann, Photocatalytic degradation of different chromophoric dyes in aqueous phase using La and Mo doped TiO₂ hybrid carbon spheres, *J. Alloys Compd.*, 632 (2015) 837–844.
- [33] L.G. Devi, S.G. Kumar, Influence of physicochemical–electronic properties of transition metal ion doped polycrystalline titania on the photocatalytic degradation of Indigo Carmine and 4-nitrophenol under UV/solar light, *Appl. Surf. Sci.*, 257 (2011) 2779–2790.
- [34] S. Kim, S.-J. Hwang, W. Choi, Visible light active platinum-ion-doped TiO₂ photocatalyst, *J. Phys. Chem. B*, 109 (2005) 24260–24267.
- [35] F. B. Li, X.Z. Li, Photocatalytic properties of gold/gold ion-modified titanium dioxide for wastewater treatment, *Appl. Catal., A*, 228 (2002) 15–27.
- [36] L.G. Devi, N. Kottam, S.G. Kumar, Preparation and characterization of Mn-doped titanates with a bicrystalline framework: correlation of the crystallite size with the synergistic effect on the photocatalytic activity, *J. Phys. Chem. C*, 113 (2009) 15593–15601.
- [37] L.G. Devi, B.N. Murthy, S.G. Kumar, Photocatalytic activity of TiO₂ doped with Zn²⁺ and V⁵⁺ transition metal ions: influence of crystallite size and dopant electronic configuration on photocatalytic activity, *Mater. Sci. Eng., B*, 166 (2010) 1–6.
- [38] Y. Fu, T. Viraraghavan, Fungal decolorization of dye wastewaters: a review, *Bioresour. Technol.*, 79 (2001) 251–262.